Wideband Self-Decoupled Slot MIMO Antennas with Two Transmission Zeros

Xing Yuan, Cuixia Huang, *Student Member, IEEE*, Jiangwei Sui, *Member, IEEE*, Yi-Feng Cheng, *Member, IEEE*, Xiaohu Fang, *Senior Member, IEEE*, and Xiangwei Zhu

***Abstract*—A self-decoupled wideband slot MIMO antenna pair is proposed in this letter. The two slot antennas are bent into two perpendicular portions, and the current directions on one portion of the two antennas are the same and those on the other ones are opposite to make the total current coupling cancel out with each other, so the first transmission zero is achieved. To widen the decoupling bandwidth, another short-ended slot is introduced around the center point of the original slot antenna to maintain the first transmission zero. Based on the same current coupling cancellation mechanism, a second transmission zero can be generated at this higher frequency, so a wideband self-decoupled MIMO antenna design is achieved. One two-element demonstrational example working in the N78 band (3.3 – 3.8GHz) is simulated and measured. The results show that the proposed slot antennas achieve isolation of better than 20 dB and matching conditions of better than -10 dB within the N78 band. Besides, the envelope correlation coefficient (ECC) is less than 0.006, and the average total efficiency is about 80%. Another four-element linear array is also designed and measured to justify the generality of the proposed method.**

***Index Terms*—Antenna decoupling, MIMO antennas, self-decoupled, slot antennas, wideband.**

I. Introduction

MULTI-INPUT AND MULTI-OUTPUT (MIMO) antennas have been vital modules in modern wireless communication systems to provide high data throughput. However, the mutual coupling between MIMO antennas becomes much severer with antenna separation decreases, which greatly deteriorates the antenna performance and the eventual data rate [1]. To reduce the antenna mutual coupling, many efforts have been devoted in recent decades, such as using neutralization lines [2], parasitic elements [3], decoupling networks [4], and so on. Some wideband decoupling structures are also proposed to enhance the working bandwidth, such as bent slots [5], neutralization lines [6] – [8], decoupling circuits [9], [10], parasitic elements [11], shorting stubs [12], coupled co-planar waveguide (CPW) [13], just name a few. Although these methods can achieve low mutual coupling across a wide band, they all require an extra decoupling structure, which will increase the antenna's total footprint.

In recent years, the self-decoupled concept is proposed to reduce mutual coupling without introducing any extra decoupling structure. Firstly, the antenna configuration can be tactically designed to achieve natural high isolation, such as asymmetrically placed loop antennas [14] and two inverted-F antennas by tuning the branch geometry and dimensions [15]. The common mode and differential mode of the antenna system can also be adjusted to cancel with each other by tuning the feeding position [16], feeding structure [17], and ground size [18]. Besides, two antennas can be self-decoupled using orthogonal features, such as orthogonal modes [19] – [22], orthogonal polarizations [23], [24], and orthogonal patterns [25]. And in [26], a wideband self-decoupled MIMO antenna design is achieved by exciting two differential modes and two common modes within the working bands. Nevertheless, a Balun chip is inserted into the feeding network to excite the differential modes, which will sacrifice the antenna efficiency. Very recently, the self-multipath concept is proposed to obtain a wideband decoupling with multiple transmission zeros [27]. Besides, the spatial and polarization diversity can also be directly utilized to achieve a wideband high-isolated design with multi-mode antenna elements [28].

In this letter, a self-decoupled wideband slot MIMO antenna pair with two transmission zeros is proposed. By appropriately bending the structure of two traditional slot antennas, the currents in one portion of the two antennas are of the same direction and those in other portions are of opposite directions, so a transmission zero can be achieved by tuning these two couplings to cancel out with each other. To generate a second transmission zero, another short-ended L-shaped slot portion is inserted around the center point of the main slot, where the first transmission zero is maintained. Based on the same coupling cancellation mechanism, a second transmission zero is achieved. Moreover, the proposed current cancellation scheme can be straightforwardly adopted in a linear array design, where the adjacent element pair can be naturally self-decoupled.

Manuscript received xxxx xx, 2023; accepted xxxx. This work was supported in part by the National Key R&D Program of China under Grant 2021YFA0716500, and by the National Natural Science Foundation of China under Grant 62201625, 62001525, and 62201183. (*Corresponding author: Jiangwei Sui.*)

Xing Yuan, Cuixia Huang, Jiangwei Sui, and Xiangwei Zhu are with the School of Electronics and Communication Engineering, Shenzhen Campus of Sun Yat-sen University, Shenzhen 518000, China (e-mail: yuanx26@mail2.sysu.edu.cn; huangcx7@mail2.sysu.edu.cn; suijw@mail.sysu.edu.cn; zhuxw666 @mail.sysu.edu.cn).

Yi-Feng Cheng is with the School of Electronics and Information, Hangzhou Dianzi University, Hangzhou 310018, China (e-mail: chengyifeng2013@gmail.com).

Xiaohu Fang is with the School of Micro-electronics, Southern University of Science and Technology, Shenzhen 518000, China (email: fangxh@sustech.edu.cn).

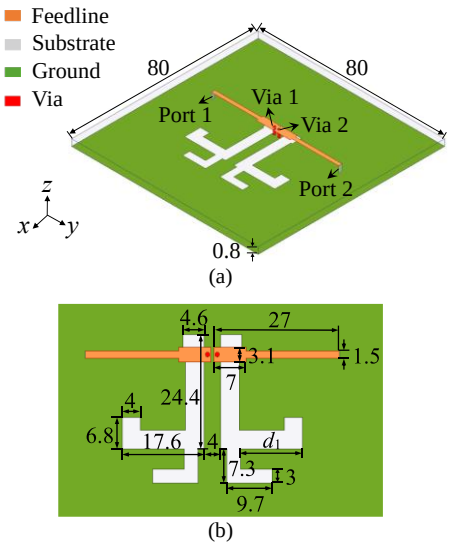

Fig. 1. Configuration of the proposed wideband slot MIMO antennas. (a) Perspective view. (b) Zoom-in view. The unit used here is mm.

II. Antenna Configuration and Operating Mechanism

A. Configuration of the Proposed Antenna

Fig. 1 illustrates the geometry of the proposed wideband slot antennas with two symmetrical antenna elements back-to-back placed. On a 0.8-mm FR4 substrate with a relative dielectric constant of 4.3 and a loss tangent of 0.02, the wideband slot antennas are constructed. Each antenna is composed of a primary L-shaped radiating element and another L-shaped short-ended stub. Two microstrip feeding lines are symmetrically placed on the upper side of the substrate and positioned near the uppermost portion of the primary radiating element with one end shorted to the ground plane through a metal via, as the red dot denotes in Fig. 1(a). And The specific dimension parameters are marked in Fig. 1(b).

B. Decoupling Mechanism

The antenna evolution diagram is depicted in Fig. 2. At first, two slot antennas are parallel arranged, which is denoted as the reference antennas, as is shown in Fig. 2(a). Due to the same current directions of the two slot antennas, there exists strong mutual coupling, as the -6 dB S_{21} proved in Fig. 3. To reduce the mutual coupling, the straight slot is bent as an L-shaped one, which is denoted as the case 1 in Fig. 2(b). For the vertical portion, whose current is marked as I_1 in Fig. 4, the directions of the two currents for the two ports' excitement are the same. Differently, for the horizontal portion, whose current is marked as I_2, the current directions for the two ports are opposite. Therefore, the coupling coefficients for the two portions, k_1 and k_2, are of opposite characteristics. As the S-parameters justify in Fig. 3, there generates a transmission zero at 3.5 GHz for case 1, and the mutual coupling is reduced from -6 dB to lower than -20 dB at 3.5 GHz compared to the reference one.

However, the bandwidth for the isolation and matching is not enough for some application scenarios, for example, the wider N78 band for global communication, which is from 3.3 to 3.8 GHz. Inspired by the coupling cancellation mechanism analyzed in the first transmission zero, an extra L-shaped

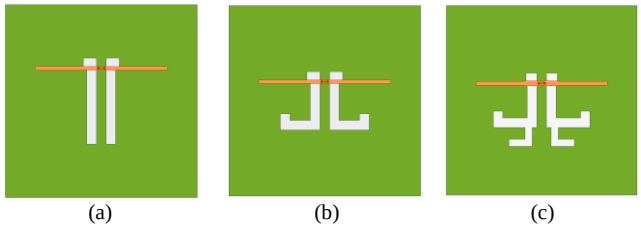

Fig. 2. Evolution process of the antenna pair. (a) Reference antennas. (b) Case 1. (c) Case 2 (proposed).

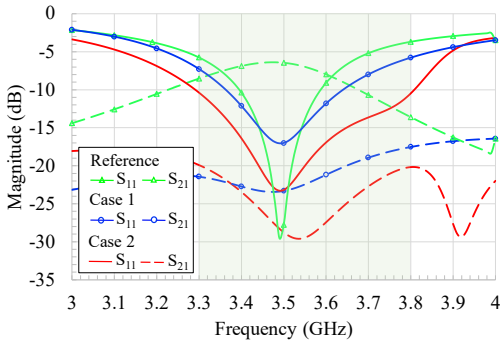

Fig. 3. Simulated S-parameters of the reference antennas and the two cases.

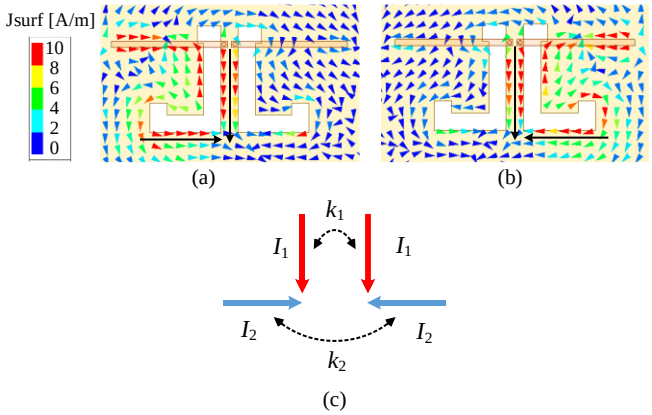

Fig. 4. Simulated current distributions of case 1 at 3.5 GHz and the decoupling scheme. (a) Port 1 excited. (b) Port 2 excited. (c) Decoupling Scheme.

portion is introduced around the center point of the original L-shaped slot antenna in case 1, as is shown in Fig. 2(c), which is marked as case 2. And the introduced L-shaped portion mainly has two effects, introducing a second transmission zero to enhance the isolation bandwidth, and introducing a second mode to enhance the impedance bandwidth, as can be observed from Fig. 3. As shown in Fig. 5, the loading position of the portion greatly influences the original resonant mode. The initial resonance point shifts to lower frequencies as d_1 decreases, reflecting the fact that the farther the loaded portion is from the current zero point, the greater the effect on the original transmission zero.

The current distribution at 3.5 GHz with port 1 excited is first studied, which is similar to that in Fig. 4(a), so the decoupling effect is maintained. Moreover, there generates a second transmission zero at 3.92 GHz in addition to 3.5 GHz. To study the decoupling mechanism of the second transmission zero, the current distributions of the two ports at 3.92 GHz are plotted in Figs. 6(a) and (b). Differently from those of 3.5 GHz, for 3.92 GHz, when port 1 is excited, the main currents locate on the

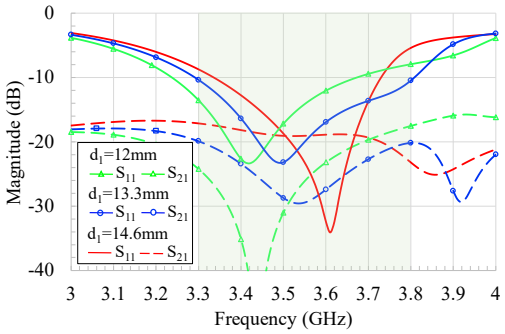

Fig. 5. Simulated S-parameters with different d_1 in the proposed antenna.

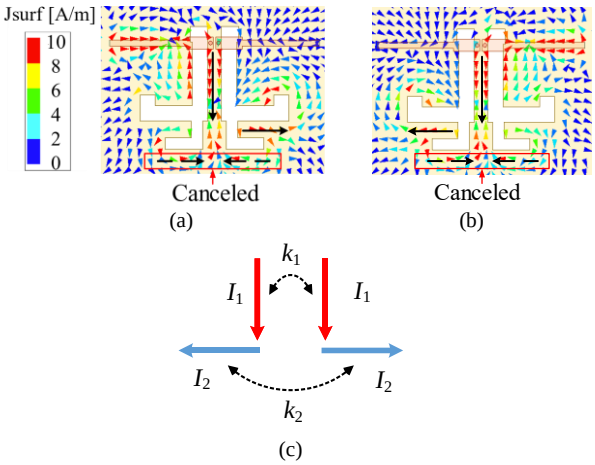

Fig. 6. Simulated current distributions of the proposed antennas at 3.92 GHz and the decoupling scheme. (a) Port 1 excited. (b) Port 2 excited. (c) Decoupling Scheme.

vertical portion and the right horizontal portion, and the scenario is similar for port 2. Therefore, based on the same coupling cancellation mechanism, a similar decoupling scheme can be obtained in Fig. 6(c). One different point is that I_1 and I_2 are out of phase at 3.5 GHz, meaning that it is a loop mode, while at 3.92 GHz, the two currents are in phase, meaning that it is a quasi-dipole mode. This difference will be found from the radiation patterns of the two frequencies, as illustrated in Fig. 7. It is observed that although there are both certain radiations on the x-o-z and y-o-z planes for the two modes, the stronger radiation for the first mode is along the x-o-z plane, while that for the second mode is along the y-o-z plane.

III. Results and Discussion

The demonstrational example discussed in Part II is fabricated, as is shown in Fig. 8. It is seen from Fig. 9 that there exist two transmission zeros, and the impedance matching is better than -10 dB with port isolation greater than 20 dB.

And the radiation performance is further studied. As is shown in Fig. 10, the measured average total efficiency is about 80 % throughout the N78 band, which is quite good taking into consideration the high loss of the FR4 substrate, and a higher value can be expected if a low loss substrate is utilized. And for MIMO antennas, it is well-known that the envelope correlation coefficient (ECC) is an important parameter to evaluate the spatial correlation of the two antennas, which can be calculated from the measured complex far-field electric fields. The

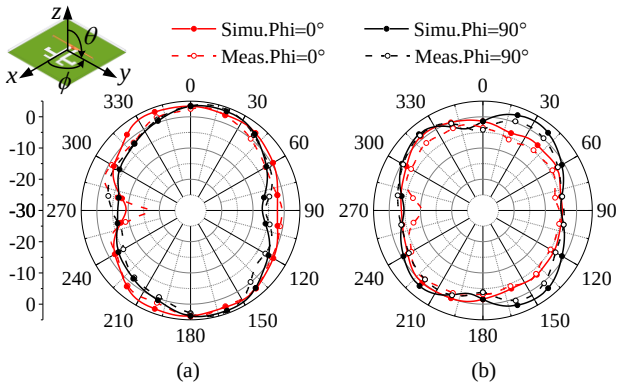

Fig. 7. Simulated and measured radiation patterns of the antenna with port 1 excited. (a) At 3.55 GHz. (b) At 3.87 GHz.

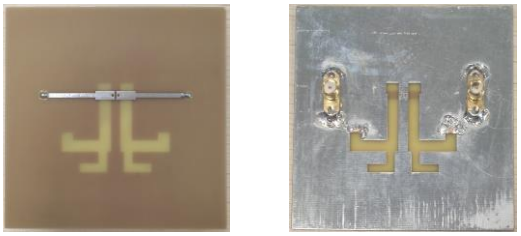

Fig. 8. Pictures of the prototyped two-element antennas. (a) Top view. (b) Bottom view.

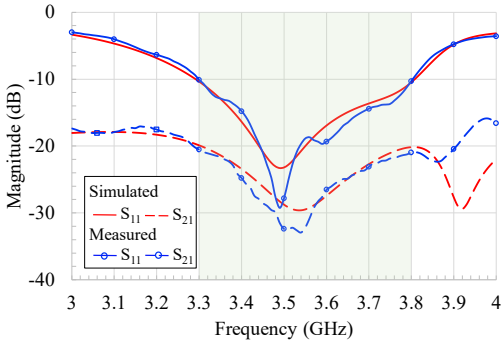

Fig. 9. Simulated and measured S-parameters of the proposed antenna.

calculated ECC is also presented in Fig. 10, showing that the ECC is less than 0.006 in the operating band.

To justify the generality, a four-element slot linear array is constructed in Fig. 11. By properly adjusting the geometry and size of two short-ended slots, the mutual coupling between Ant 2 and Ant 3 can also be eliminated simultaneously based on the same current cancellation scheme. As is observed from Fig. 12, although the antenna separation is only 5 mm (0.055 λ_0 at 3.3 GHz), all the mutual couplings are smaller than -17.7 dB across the N78 band with impedance matching better than -10 dB. As expected, the proposed current cancellation scheme can be applied to high-order linear arrays with many more elements. And Fig. 13 presents the top and bottom views of the prototyped array.

One thing that should be discussed is the potential application scenarios. For sub-6 GHz applications, it may be used in the wireless access point system, such as the hot-sport devices (MiFi). For millimeter-wave applications, the slot antenna is a competitive candidate due to its low cost and easy implementation feature. And the proposed scheme may be adopted in linear antenna arrays in Radar systems and future

TABLE I
COMPARISON OF SOME STATE-OF-THE-ART HIGH-ISOLATED MIMO ANTENNAS

Ref.	Self-Decoupled	Linear Array Capability*	Impedance Bandwidth (%, -10 dB)	Isolation (dB)	Radiation Pattern	Total Antenna Size ($\lambda_0 \times \lambda_0$)**	Antenna Separation (λ_0)	Total Efficiencies (%)
[9][2020]	No	No	5.7 (3.4 – 3.6)	>25	Dual-beam	0.57 × 0.48	0.13	> 80
[10][2017]	No	No	8.1 (2.35 – 2.55)	>20	Omnidirectional	0.18 × 0.08	0.07	45 – 52.5
[13][2023]	No	No	65.5 (3.7 – 7.3)	>20	Unidirectional	1.25 × 0.68	0.1	> 87
[15][2020]	Yes	No	14.1 (3.3 – 3.8)	>20	Unidirectional	0.49 × 0.18	0.024	75 – 85
[17][2022]	Yes	No	2.1 (4.8 – 4.9)	>25	Unidirectional	0.25 × 0.25	0.1	> 83
[25][2020]	Yes	Yes	4.1 (2.4 – 2.5)	>20	Omnidirectional	0.49 × 0.21	0.03	77 – 85
Proposed	Yes	Yes	14.1 (3.3 – 3.8)	>20	Dual-beam	0.46 × 0.37	0.047	72 – 90

* Here the linear array denotes that the separations of all the adjacent elements are comparable and small enough.
** Here λ_0 denotes the wavelength at the center frequency in free space.

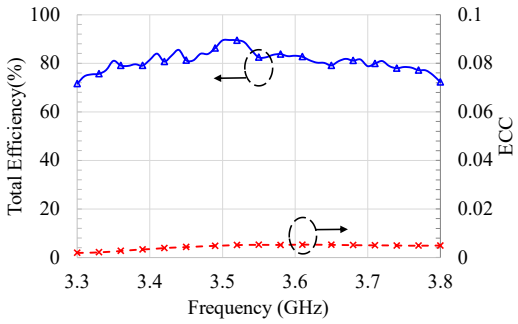

Fig. 10. Measured total efficiency and ECC of the proposed antennas.

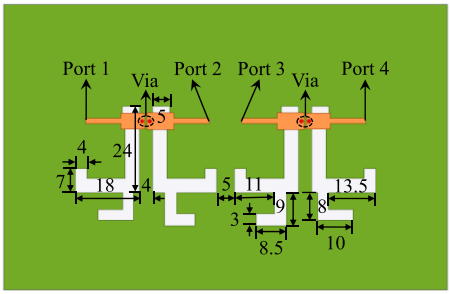

Fig. 11. Configuration of the four-element linear array.

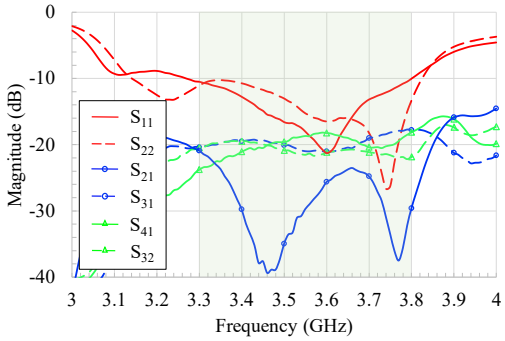

Fig. 12. Measured S-parameters of the four-element linear array.

mobile terminals.

A comparison of the proposed MIMO antennas with the existing ones is conducted in Table I. It is seen that for the antennas in [9], [10], [17], and [25], the bandwidth is somewhat not too wide. Although the antennas in [13] and [15] present high isolation within a wide band, both of these designs are based on the pair scheme, which means that the decoupling is achieved within two antennas, and a pair can be set as a basic unit to form a multi-element design, where the distance between two units is usually far enough to reduce the inter-unit mutual couplings. Therefore, these methods cannot be directly utilized to design a linear array, in which the separations of all the adjacent elements are comparable and quite small, for example, the adjacent separations in the proposed array are 4 mm, 5 mm, and 4 mm, respectively. For the proposed one, two transmission zeros are achieved using current cancellations, and no balanced feeding is required. And the proposed current cancellation scheme can be straightforwardly adopted in a linear array with multiple antenna elements, which makes it stand out from the existing decoupling methods.

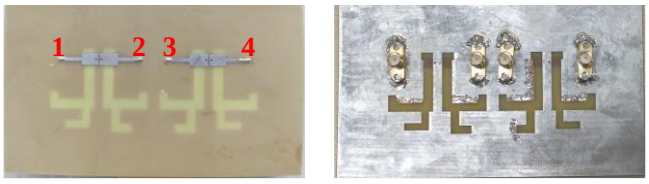

(a) (b)

Fig. 13. Pictures of the prototyped four-element linear array. (a) Top view. (b) Bottom view.

IV. CONCLUSION

This letter presents a self-decoupled wideband slot MIMO antenna pair using coupling cancellations. By bending the traditional straight slot antennas L-shaped, the current couplings on the two portions of the L-shaped slot are opposite, so a first transmission zero is generated by tuning the dimensions of the two portions. To introduce a second transmission zero, another short-ended L-shaped slot is designed around the center point of the main slot using the same coupling cancellation mechanism. Moreover, the impedance-matching performance of the slot antennas is improved by introducing a quasi-dipole mode. And the proposed current cancellation scheme can be easily extended to a linear array with more than two elements.

REFERENCES

[1] X. Chen, S. Zhang, and Q. Li, "A review of mutual coupling in MIMO systems," *IEEE Access*, vol. 6, pp. 24706–24719, 2018.

[2] A. Diallo, C. Luxey, P. Le Thuc, R. Staraj, and G. Kossiavas, "Study and reduction of the mutual coupling between two mobile phone PIFAs operating in the DCS1800 and UMTS bands," *IEEE Trans. Antennas Propag.*, vol. 54, no. 11, pp. 3063–3074, Nov. 2006.

[3] L. Zhao and K.-L. Wu, "A decoupling technique for four-element symmetric arrays with reactively loaded dummy elements," *IEEE Trans. Antennas Propag.*, vol. 62, no. 8, pp. 4416–4421, Aug. 2014.

[4] M. Li, L. Jiang, and K. L. Yeung, "Novel and efficient parasitic decoupling network for closely coupled antennas," *IEEE Trans. Antennas Propag.*, vol. 67, no. 6, pp. 3574–3585, Jun. 2019.

[5] J.-F. Li, Q.-X. Chu, and T.-G. Huang, "A compact wideband MIMO antenna with two novel bent slits," *IEEE Trans. Antennas Propag.*, vol. 60, no. 2, pp. 482-489, Feb. 2012.

[6] Y. Wang and Z. Du, "A wideband printed dual-antenna with three neutralization lines for mobile terminals," *IEEE Trans. Antennas Propag.*, vol. 62, no. 3, pp. 1495–1500, Mar. 2014.

[7] S. Zhang and G. F. Pedersen, "Mutual coupling reduction for UWB MIMO antennas with a wideband neutralization line," *IEEE Antennas Wireless Propag. Lett.*, vol. 15, pp. 166–169, 2016.

[8] C.-D. Xue, X. Y. Zhang, Y. F. Cao, Z. Hou, and C. F. Ding, "MIMO antenna using hybrid electric and magnetic coupling for isolation enhancement," *IEEE Trans. Antennas Propag.*, vol. 65, no. 10, pp. 5162–5170, Oct. 2017.

[9] Y.-F. Cheng and K.-K. M. Cheng, "Compact wideband decoupling and matching network design for dual-antenna array," *IEEE Antennas Wireless Propag. Lett.*, vol. 19, no. 5, pp. 791–795, May 2020.

[10] S. N. Venkatasubramanian, L. Li, A. Lehtovuori, C. Icheln, and K. Haneda, "Impact of using resistive elements for wideband isolation improvement," *IEEE Trans. Antennas Propag.*, vol. 65, no. 1, pp. 52–62, Jan. 2017.

[11] Y. Q. Hei, J. G. He, and W. T. Li, "Wideband decoupled 8-element MIMO antenna for 5G mobile terminal applications," *IEEE Antennas Wireless Propag. Lett.*, vol. 20, no. 8, pp. 1448–1452, Aug. 2021.

[12] X.-T. Yuan, Z. Chen, T. Gu, and T. Yuan, "A wideband PIFA-pair-based MIMO antenna for 5G smartphones," *IEEE Antennas Wireless Propag. Lett.*, vol. 20, no. 3, pp. 371–375, Mar. 2021.

[13] Z. Zhou, Y. Ge, J. Yuan, Z. Xu, and Z. D. Chen, "Wideband MIMO antennas with enhanced isolation using coupled CPW transmission lines," *IEEE Trans. Antennas Propag.*, vol. 71, no. 2, pp. 1414-1423, Feb. 2023.

[14] K.-L. Wong, C.-Y. Tsai, and J.-Y. Lu, "Two asymmetrically mirrored gap-coupled loop antennas as a compact building block for eight-antenna MIMO array in the future smartphone," *IEEE Trans. Antennas Propag.*, vol. 65, no. 4, pp. 1765–1778, Apr. 2017.

[15] J. Sui and K.-L. Wu, "A self-decoupled antenna array using inductive and capacitive couplings cancellation," *IEEE Trans. Antennas Propag.*, vol. 68, no.7, pp. 5289-5296, Jul. 2020.

[16] L. Sun, Y. Li, Z. Zhang, and H. Wang, "Self-decoupled MIMO antenna pair with shared radiator for 5G smartphones," *IEEE Trans. Antennas Propag.*, vol. 68, no. 5, pp. 3423-3432, May 2020.

[17] A. Zhang, K. Wei, Y. Hu, and Q. Guan, "High-isolated coupling-grounded patch antenna pair with shared radiator for the application of 5G mobile terminals, " *IEEE Trans. Antennas Propag.*, vol. 70, no. 9, pp. 7896-7904, Sep. 2022.

[18] L. Sun, Y. Li, Z. Zhang, and H. Wang, "Antenna decoupling by common and differential modes cancellation," *IEEE Trans. Antennas Propag.*, vol. 69, no. 2, pp. 672–682, Feb. 2021.

[19] H. Li, Z. T. Miers, and B. K. Lau, "Design of orthogonal MIMO handset antennas based on characteristic mode manipulation at frequency bands below 1 GHz," *IEEE Trans. Antennas Propag.*, vol. 62, no. 5, pp. 2756–2766, May. 2014.

[20] L. Sun, H. Feng, Y. Li, and Z. Zhang, "Compact 5G MIMO mobile phone antennas with tightly arranged orthogonal-mode pairs," *IEEE Trans. Antennas Propag.*, vol. 66, no. 11, pp. 6364–6369, Nov. 2018.

[21] H. Xu, S. S. Gao, H. Zhou, H. Wang, and Y. Cheng, "A highly integrated MIMO antenna unit: differential/common mode design," *IEEE Trans. Antennas Propag.*, vol. 67, no. 11, pp. 6724-6734, Nov. 2019.

[22] A. Ren, Y. Liu, and C.-Y.-D. Sim, "A compact building block with two shared-aperture antennas for eight-antenna MIMO array in metal-rimmed smartphone," *IEEE Trans. Antennas Propag.*, vol. 67, no. 10, pp. 6430–6438, Oct. 2019.

[23] M.-Y. Li et al., "Eight-port orthogonally dual-polarized antenna array for 5G smartphone applications," *IEEE Trans. Antennas Propag.*, vol. 64, no. 9, pp. 3820–3830, Sep. 2016.

[24] L. Chang, Y. Yu, K. Wei, and H. Wang, "Polarization-orthogonal co-frequency dual antenna pair suitable for 5G MIMO smartphone with metallic bezels," *IEEE Trans. Antennas Propag.*, vol. 67, no. 8, pp. 5212–5220, Aug. 2019.

[25] Y.-F. Cheng and K.-K. M. Cheng, "Decoupling of two-element printed-dipole antenna array by optimal meandering design," *IEEE Trans. Antennas Propag.*, vol. 68, no.11, pp.7328–7338, Nov. 2020.

[26] L. Sun, Y. Li, Z. Zhang, and Z. Feng, "Wideband 5G MIMO antenna with integrated orthogonal-mode dual-antenna pairs for metal-rimmed smartphones," *IEEE Trans. Antennas Propag.*, vol. 68, no. 4, pp. 2494-2503, Apr. 2020.

[27] A. Zhang, K. Wei, and Z. Zhang, "Multiband and wideband self-multipath decoupled antenna pairs," *IEEE Trans. Antennas Propag.*, vol. 71, no. 7, pp. 5605-5615, Jul. 2023.

[28] A. Ren, H. Yu, L. Yang, Z. Huang, Z. Zhang, and Y. Liu, "A broadband MIMO antenna based on multimodes for 5G smartphone applications," *IEEE Antennas Wireless Propag. Lett.*, vol. 22, no. 7, pp. 1642-1646, Jul. 2023.